Analysis of Hybrid Optoelectronic WDM ADC

Payam Rabiei and A. F. J. Levi

Abstract—**A new hybrid optoelectronic wavelength-division demultiplexed (WDM) architecture to extend electronic analog-to-digital conversion (ADC) performance is analyzed and simulated. Mode-locked optical pulses are amplitude-modulated by an RF signal and optically demultiplexed into a number of parallel channels. The signal in each channel is converted to an electrical signal and then passed through a simple low-pass filter. The effect of low-pass filter response, filter matching, noise due to jitter, and detector shot noise on system performance is simulated.**

Index Terms—**Analog-to-digital conversion (ADC), digital signal processing, mode-locked laser, radio frequency (RF) mixer.**

I. INTRODUCTION

THE USE of fiber-optic technology to improve the performance of analog-to-digital converters (ADCs) has been pursued for many years [1]. Recently, interest in this subject has been heightened with the introduction of hybrid optoelectronic techniques such as optical time-stretching [2] and wavelength-division demultiplexed (WDM) sampling [3]. The basic idea is to optoelectronically process the radio frequency (RF) signals to generate lower bandwidth signals that can be sampled using electronic ADCs. Digital signal processing (DSP) is then used to reconstruct the original signal.

In the WDM experiments [3], Kang and Esman use a single mode-locked laser and WDM generator to produce a wavelength time-interleaved pulsed optical carrier with high optical pulse repetition rate. The time-interleaved multiple-wavelength optical pulse-train is amplitude-modulated at RF using an integrated electrooptic modulator and the resulting output is then wavelength-demultiplexed into separate channels. In this way, the optical pulse repetition rate on each channel is reduced. Each channel has an optoelectronic receiver whose electrical output is fed to an electronic ADC. Kang and Esman envisioned that, in a complete system, the digital output of each individual channel would be processed to reconstruct the original RF signal.

The purpose of this paper is to analyze a WDM sampler architecture and DSP system for the case of limited optoelectronic receiver bandwidth. In this situation, the complete hybrid system acts as an optically assisted RF mixer whose output is a number of low-frequency signals which are digitized using relatively low sampling rate ADCs. These signal components have known relative time delay so that a DSP can be used to recover the original high-frequency RF signal.

II. SYSTEM ARCHITECTURE

We consider a system, which uses a pulsed multiwavelength optical source, an electrooptic modulator, an optical wavelength demultiplexer, optical detectors, electronic filters, electronic ADCs, and a DSP as shown in Fig. 1 The source generates time-interleaved optical pulses of n different center wavelengths [4], [5]. It is important to note that the optical pulse repetition rate of *each wavelength* is a factor of n smaller than the sampling rate. The optical pulses are amplitude-modulated by the RF input signal in the electrooptic modulator portion of the system. For illustrative purposes $X(\omega_{\mathrm{RF}})$ is a triangle whose highest frequency component is $\omega_{\mathrm{RF\,max}}$. The optical pulses are then wavelength-demultiplexed to a lower pulse repetition rate using an array waveguide grating (AWG). Each of the n different optically demultiplexed signal channels is then delayed and converted to an electrical signal by a high-responsivity detector. The delay is incorporated in each channel so that different ADCs may be synchronized using a single clock. The electric current flowing in each detector is proportional to the energy in the optical pulse. Each electrical signal is low-pass filtered before electronic analog-to-digital conversion. The low-pass filter (LPF) bandwidth is up to a factor of n smaller than the RF signal bandwidth. An advantage of this scheme is that electronic ADCs with relatively low input bandwidth can be used to sample very-broad-band RF signals. For a given signal bandwidth (BW) and ADC sampling rate (f_s) the minimum number of channels used by the system is

$$n = \frac{2\mathrm{BW}}{f_s}.$$

This is the Nyquist theorem, which assumes a perfect step-function low-pass input-filter frequency response. Clearly, if we wished to sample a 20-GHz RF signal to 8-b resolution using electronic ADCs with 8 GS/s and 8-b resolution we would need a *minimum* of 5 ADC channels. In practice the number of channels will be greater to accommodate the fact that the LPFs and other system components are not ideal.

However, by using a DSP it is possible to reconstruct the original RF signal from the multiple low-speed digitally sampled signals.

III. SYSTEM ANALYSIS

In this section we will analyze the system and obtain the transfer function. We show that the low-pass filtered signals contain all the information required to reconstruct the original RF signal.
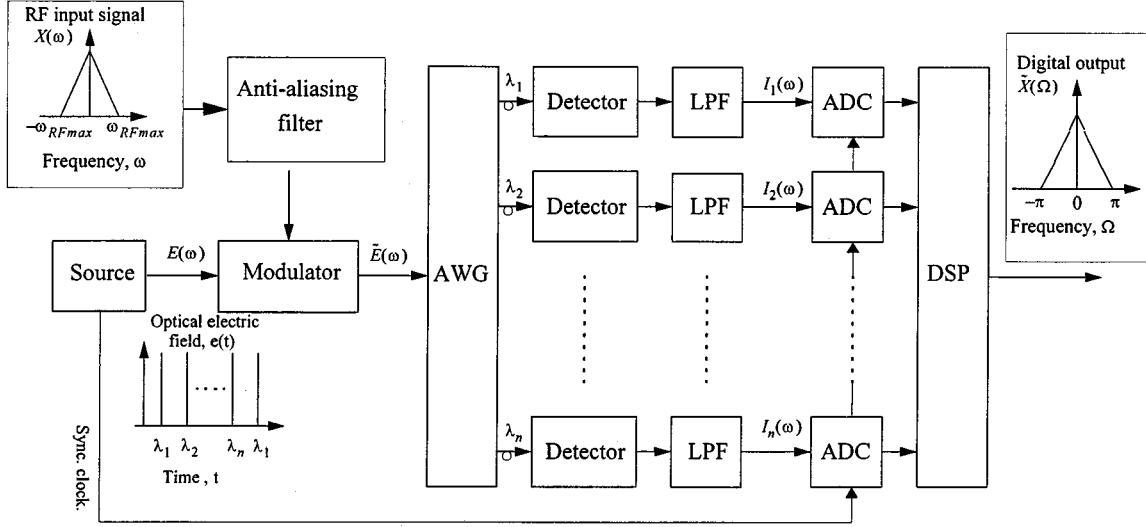
Fig. 1. Schematic diagram of the hybrid optoelectronic WDM ADC system architecture. The optical multiwavelength source is RF-modulated and demultiplexed using an array waveguide grating (AWG). The output of the AWG is detected, low-pass filtered, and quantized. DSP reconstructs the original signal.

The optical source is an external cavity mode-locked laser which generates optical pulses of different center wavelength λ_m. Each optical pulse centered at λ_m consists of $N+1$ external cavity modes where N is an integer. The time-varying electric field centered at λ_m is given by [6] (assuming nonequal power in each mode)

$$e_m(t) = \sum_{k=-N/2}^{N/2} a_{m,k} e^{j(\omega_m + k\omega_C)t}, \qquad m = 1, \ldots, n.$$

The subscript m labels different channels with different center wavelengths λ_m and corresponding optical frequency ω_m. k labels the modes that are locked together around each center wavelength λ_m. The mode spacing of the external cavity is ω_C which also corresponds to the pulse repetition time $t_C = 2\pi/\omega_C$. $a_{m,k}$ is the amplitude of the mode k associated with center frequency ω_m. In the system, the mode spacing is chosen to be equal to the ADC sampling rate.

The optical pulses are amplitude-modulated by applying an electrical RF signal $x(t)$ to the electrooptic modulator. Assuming small-signal modulation, the modulated electric field of the optical signal is [6]

$$\hat{e}_m(t) = \sum_{k=-N/2}^{N/2} a_{m,k} \sin\left(\frac{\pi}{4} + \frac{d}{2}\right) \cdot x\left(t - \frac{mt_c}{n}\right) e^{j(\omega_m + k\omega_C)t}$$

where d is the modulation depth. For simplicity and ease of explanation, the time delay in the interleaved optical pulses is replaced with an equivalent delay in the input signal. This delay is mt_C/n. The optical pulses are then wavelength-demultiplexed into n channels and the optical signal in each channel is detected using a photodetector. Since the detector current is proportional

to the energy of the optical signal, the output of the detector is (assuming $a_{m,k} = 1$ for simplicity and assuming the modulation depth $d \ll 1$)

$$i_m(t) = \frac{1}{2}\left(1 + d \cdot x\left(t - \frac{mt_C}{n}\right)\right) \sum_{k=-N}^{N} (N - |k| + 1)e^{jk\omega_C t}$$

where $i_m(t)$ is the current of the detector m. This signal is then low-pass filtered and a signal with low-frequency components is obtained. Taking the Fourier transform of the detector current given above and multiplying the result with the LPF transfer function $H(\omega_{RF})$ one obtains

$$I_m(\omega_{RF}) = \sum_{k=-N}^{N} (N - |k| + 1)X(\omega_{RF} - k\omega_C)$$
$$\cdot e^{j((mt_C\omega_{RF} - 2\pi mk)/n)} H(\omega_{RF}).$$

$I_m(\omega_{RF})$ is the signal spectrum at the output of LPF. For simplicity, this expression neglects the constant offset value (1) and assumes $d = 1$ to avoid a delta function in the RF spectrum. It is also important to note that the mode spacing ω_C can be smaller than the Nyquist rate by a factor of n. Neglecting the phase term for the moment, this spectrum is basically the addition of the shifted (in the frequency domain) RF spectrum $X(\omega_{RF})$ multiplied by the LPF transfer function. This is shown schematically in Fig. 2 assuming a triangular shape for the input RF signal in the frequency domain and an ideal LPF, $H(\omega_{RF})$. The figure shows aliasing of signals in the output of the detector. The high-frequency components are mixed with low-frequency components. There is also a decrease in the amplitude of higher frequency bands which is due to the term $(N - |k| + 1)$.

Although there is aliasing of signals, all signal information is conserved and we can still obtain the original signal using DSP.
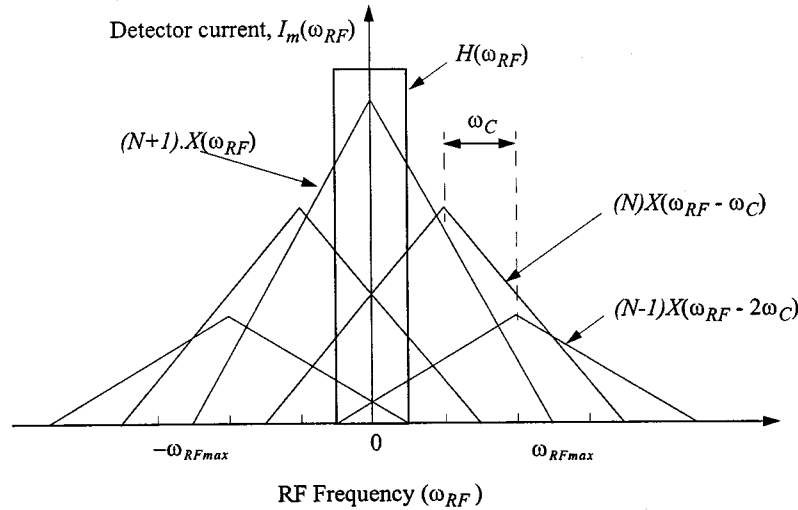
Fig. 2.   Schematic diagram of signal mixing in each detector. The high-frequency components are mixed with low-frequency components because the mode spacing ω_C is small compared to the RF bandwidth $\omega_{\mathrm{RF\,max}}$.

To show this, consider the required DSP to reconstruct the original high-frequency RF signal from the low-frequency digitized signals. The discrete Fourier transform of the sampled signal is

$$I_m(\Omega) = \frac{1}{t_C} \sum_{l=-\infty}^{\infty} \sum_{k=-N}^{N} (N - |k| + 1) X\left(\frac{\Omega}{t_c} - k\omega_C - l\omega_C\right)$$

$$\cdot e^{j((m\Omega - 2\pi m(k+l))/n)} H\left(\frac{\Omega}{t_c}\right).$$

Note that the sampling rate is identical to mode-locked laser repetition rate ω_C.

If we time-interleave the digitized samples from different channels we should be able to obtain the original signal. To mathematically model this process we insert $n - 1$ (n is the number of channels) zeros in the middle of two consecutive samples. We then delay the sample sequence by m (m is the channel number) in each channel and then add them up as shown schematically in Fig. 3 for a two-channel system. This process can be easily written in the Fourier domain as scaling the frequency, multiplying by phase term, and adding the signals

$$\hat{X}(\Omega) = \sum_{m=1}^{n} I_m(n\Omega) e^{-jm\Omega}$$

where $\hat{X}$ is the reconstructed signal. Assuming that the number of mixed signals at the LPF output is equal or less than the number of channels (which is satisfied provided that the antialiasing filter bandwidth is less than $n\omega_C/2$) we can replace N with $(n - 1)/2$ in the summation indices for $I_m(\Omega)$. By placing $I_m(\Omega)$ in the previous formula and simplifying the expression we obtain

$$\hat{X}(\Omega) = \frac{1}{t_c} \sum_{l=-\infty}^{+\infty} \left(X\left(\frac{n\Omega}{t_c} - jnl\omega_C\right) \sum_{k=-(n-1)/2}^{(n-1)/2} \right.$$

$$\left. \cdot (N - |k| + 1) H\left(\frac{n\Omega}{t_c} - (k + nl)\omega_C\right) \right)$$

for the reconstructed signal. Although it may seem complicated, this formula shows that the final reconstructed RF signal is a signal with an effective sampling rate which is n times the individual ADC sampling rate multiplied by a filter function which is the addition of shifted (in frequency domain) low-pass filter functions.

The system is equivalent to a system with an analog transfer function given by

$$T(\omega_{\mathrm{RF}}) = \sum_{k=-(n-1)/2}^{(n-1)/2} (N - |k| + 1) H(\omega_{\mathrm{RF}} - k\omega_C)$$

and whose output is digitally sampled at a rate that is n times the sampling rate of an individual electronic ADC.

It should now be clear that in this architecture the LPFs $H(\omega_{\mathrm{RF}})$ before the ADCs are not antialiasing filters. These filters should be chosen such that the transfer function of the complete system results in a flat frequency response.

We assume a system that has five channels with three locked modes in each pulse ($N + 1 = 3$). Each LPF has an identical frequency response and each ADC samples at 8 GS/s. The RF input to the electrooptic modulator has an antialiasing filter with an 18-GHz −3-dB bandwidth. Fig. 4 shows the system transfer function and low-pass filter transfer function for two-pole and eight-pole LPFs with different −3-dB bandwidths. It is clear that the system transfer function will reject some frequencies if the LPF is incorrectly designed. As an example, Fig. 4(b) shows a smooth system transfer function using a 3.8-GHz −3-dB bandwidth eight-pole Butterworth LPF. However, it is apparent from the figure that even a small change in −3-dB LPF bandwidth to 3.6 GHz introduces attenuation at 4 and 8 GHz that is undesirable.

(a)

(b)

Fig. 4. Transfer function $H(\omega_{RF})$ of the LPF and corresponding five-channel system transfer functions $T(\omega_{RF})$ for different LPF -3-dB bandwidths with three locked modes. (a) Two-pole Butterworth filters. (b) Eight-pole Butterworth filters.
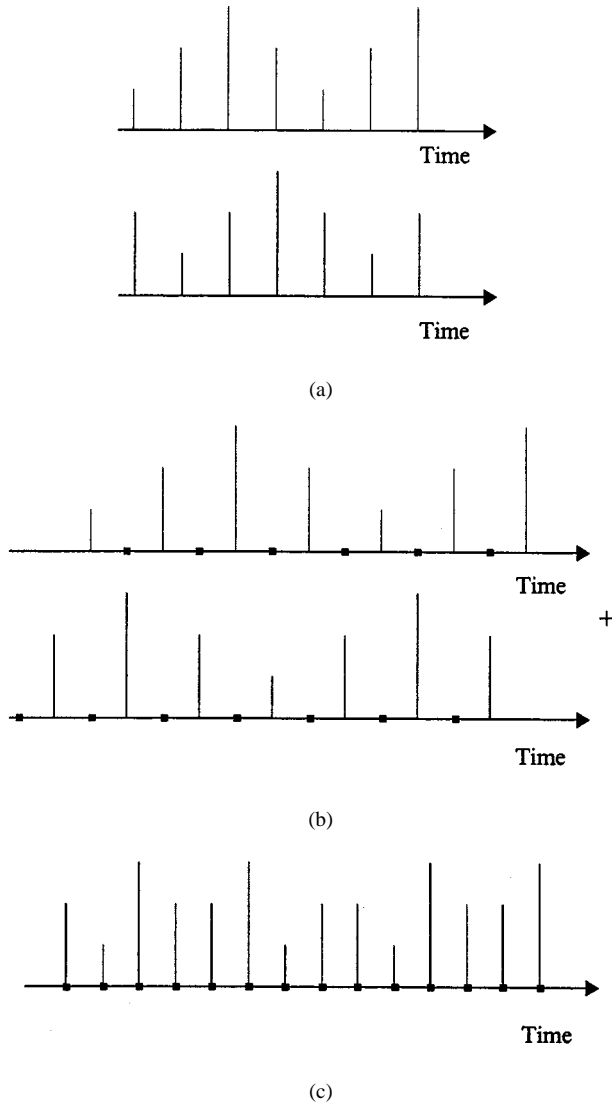

Fig. 3. Signal reconstruction method using DSP. (a) Original signals. (b) Inserting zeros and delaying. (c) Adding the signals.

The system does require that we antialias filter the RF signal prior to modulating the optical carrier. For example, if we are considering a five-channel system with 8 GS/s ADCs we sample at a 40-GS/s rate which means that, in principle, we can sample signals with frequencies up to 20 GHz and a 20-GHz antialiasing filter is required. However, due to practical limitations in filter design we do not expect to achieve operation at frequencies close to this ideal case. Compared to conventional ADCs, the effects of aliasing can also appear at relatively low frequencies near $\omega_C/2$.

We need the number of locked modes $(N + 1)$ to be at least equal to $(n - 1)/2$. This is required to have all the high-frequency components correctly mixed to low frequencies. So, for example, in a five-channel system we need at least $N + 1 = 3$. There is an advantage to having a higher number of locked modes. Looking at the term $(N - |k| + 1)$ it is clear that if $N \gg |k|$ the variation in signal amplitude in adjacent bands could be reduced. So if we have a higher number of modes locked together we will obtain a flatter frequency response. However, this
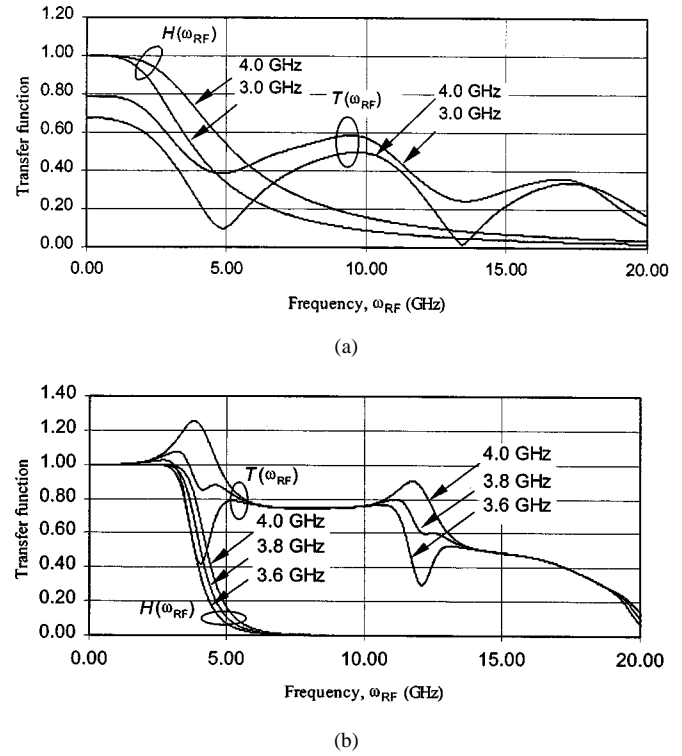
requires more optical bandwidth. Fig. 5 shows the transfer function for 100 locked modes.

The specific form of the transfer function for this system suggests that a perfect flat transfer function is obtainable if

$$H(j\omega) = \frac{1 - \exp(-j\omega t_d)}{j\omega}.$$

In this expression, t_d is the delay which must be chosen equal to t_c.

IV. OPTICAL POWER, BANDWIDTH, AND NOISE

There are different noise sources in this system. The main sources of noise are optical crosstalk in the demultiplexer, detector shot noise, and noise in the output of mode-locked laser optical source.

Optical crosstalk between different channels of the demultiplexer may be suppressed arbitrarily if the channels are chosen to be far enough apart in wavelength.

For an analog optical link it has been shown that the signal-to-noise ratio (SNR) linearly increases with the input power of the laser source [7], [8]. In the previous analysis, a very-low-noise laser source is assumed so that detector shot noise dominates.

Timing jitter can be an important source of noise in our system. Clearly, if there is timing jitter in the sampling pulses an error will be introduced in the detected optical signal and hence an error will occur in the reconstructed RF signal. The effect of jitter can be described as an equivalent amplitude
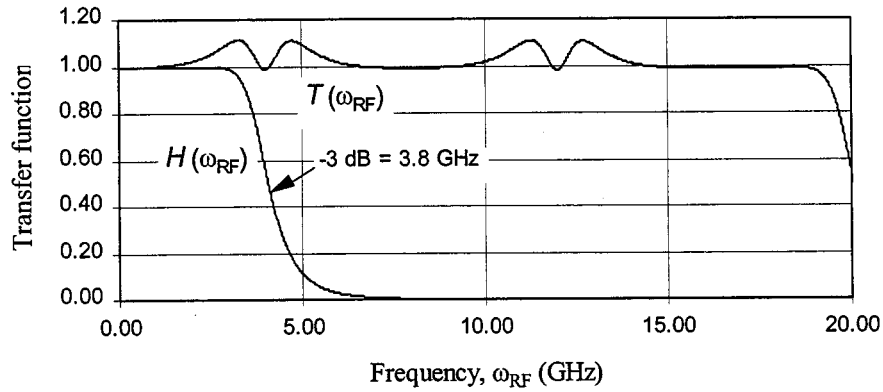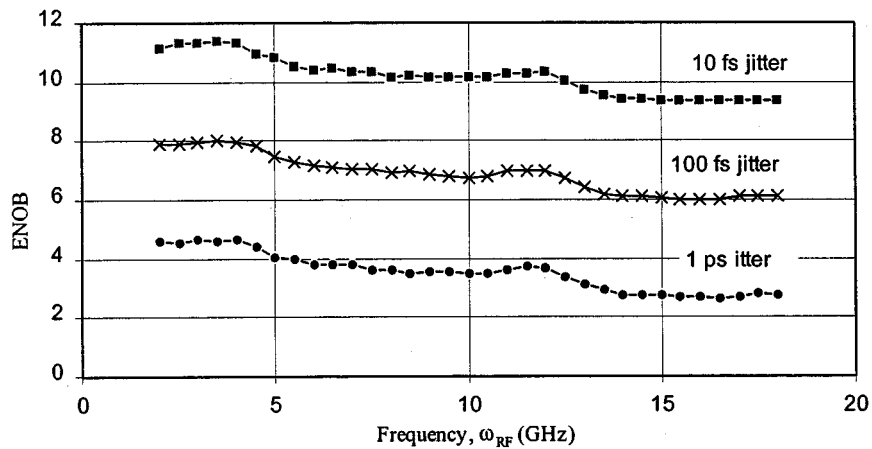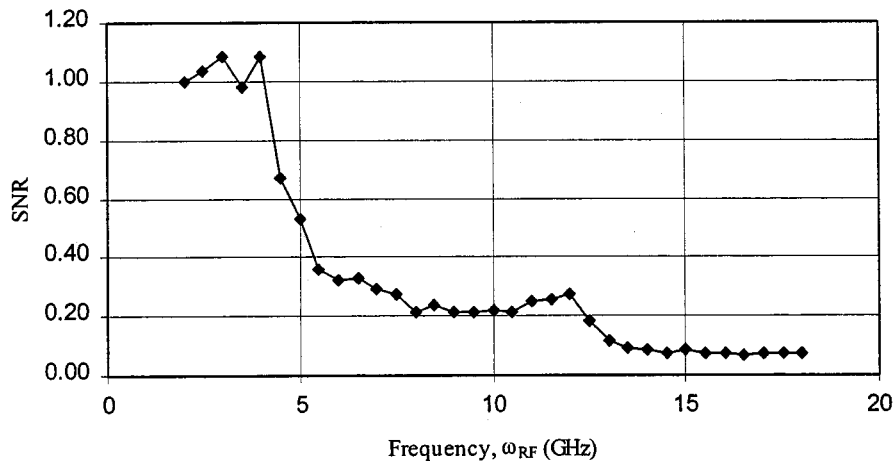
Fig. 5.   Transfer function $H(\omega_{\mathrm{RF}})$ of the LPF and corresponding five-channel system transfer functions $T(\omega_{\mathrm{RF}})$ for different LPF -3-dB bandwidths with 100 locked modes for eight-pole Butterworth filters.

(a)

(b)

Fig. 6.   Simulation results for the effect of jitter on the SNR. The five-channel system uses eight-pole Butterworth LPFs with 4-GHz -3-dB bandwidth. (a) Effective number of bits for different input optical pulse jitter. (b) SNR for 100-fs jitter plotted using normalized linear scale. The simulation assumes no shot noise.

noise. Assuming a single-tone signal at the input to our system and a timing error equal to Δt in the pulse position it may be shown that this will cause an amplitude error which is equal to

$$\frac{\Delta a}{a} = \omega_{\mathrm{RF}} \cos(\omega_{\mathrm{RF}} t) \Delta t.$$

To achieve a resolution of N_b bits we assume that the error should be less than 1/4 of the least significant bit giving
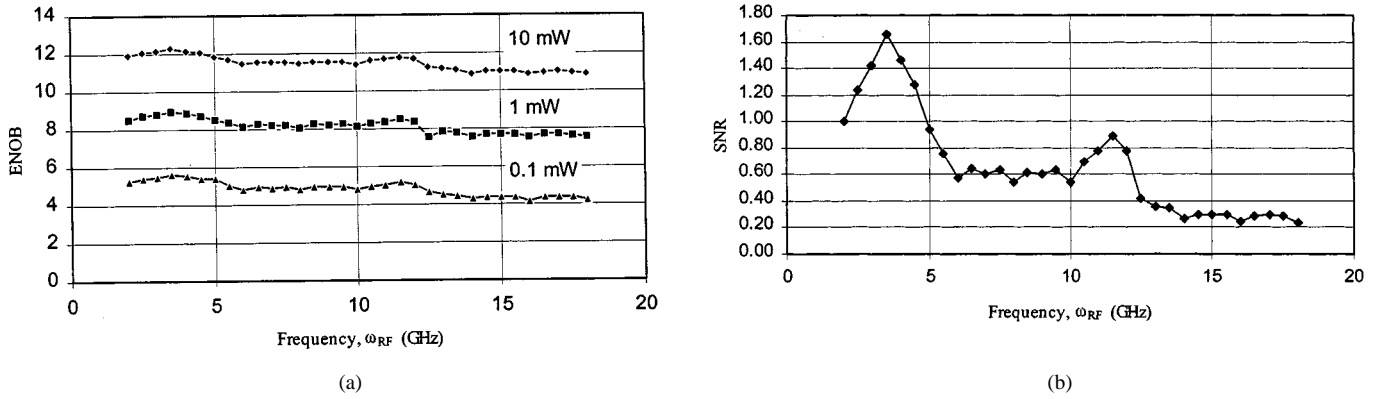
$$\Delta t < \frac{1}{2^{N_b+2} \omega_{\mathrm{RF}}}.$$

Fig. 7. Simulation results for effect of detector shot noise on SNR. The five-channel system uses eight-pole Butterworth LPFs with 4-GHz −3-dB bandwidth. (a) Shot-noise-limited ENOB for different levels of average detected optical power per channel. (b) Linear scale normalized SNR for 1-mW average detected optical power per channel. The simulation assumes no jitter.
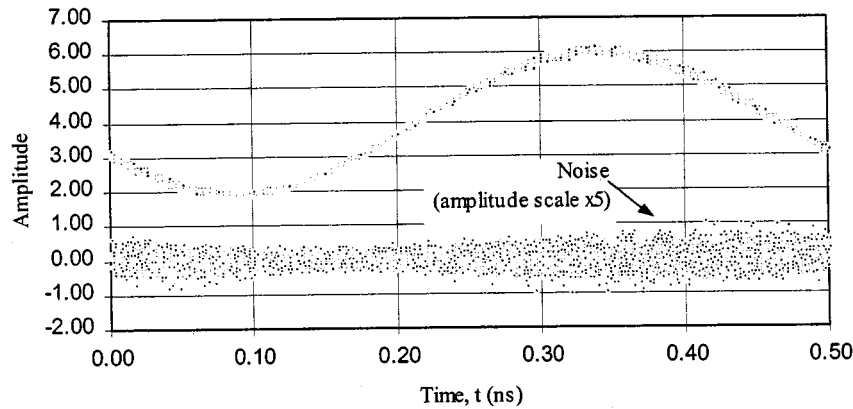

Fig. 8. Reconstructed time-domain 2-GHz signal in presence of 1-ps jitter. The five-channel system uses eight-pole Butterworth LPFs with 4-GHz −3-dB bandwidth. The simulation assumes no shot noise.

It is apparent that our system is complex and this simple analysis does not consider the effect of LPFs and other components in the system. A convenient way to analyze the noise is via numerical simulations. A numerical noise simulation has been performed for this system using Matlab software. The simulations are essentially the numerical implementation of the formulas in Section III with addition of appropriate noise terms. Simulations are performed for different input signal frequencies and the resulting SNR at the output is calculated by subtracting the resultant sampled signals from the actual input signals. For the simulations we considered optical pulses of 28-ps width (three locked modes) used in a five-channel system. The relatively long optical pulsewidth is advantageous as it reduces pulse-to-pulse amplitude noise. Shorter optical pulses will have higher number of modes locked together. For a given average optical power this results in more noise in each mode. In addition, as is well known [10], locking increasing numbers of optical modes becomes increasingly difficult and results in more amplitude and jitter noise.

The LPF used in simulations is an eight-pole Butterworth filter with a −3-dB bandwidth of 4 GHz that gives the transfer function shown in Fig. 4(b). The effect of jitter on the input pulses and also the effect of detector shot noise have been simulated. To simulate the presence of jitter, filtered Gaussian white noise is added to the temporal position of each input pulse. The

low-pass noise–filter bandwidth is chosen to be 4 GHz so that the time variation in the noise signals match the pulse repetition rate. The amplitude is chosen such that it will result in the desired root-mean square (rms) jitter value. Fig. 6(a) shows the effective number of bits (ENOB) for different input optical signal jitter. The ENOB is related to SNR via [9]

$$\text{SNR (dB)} = (6.02 \times \text{ENOB}) + 1.76.$$

Fig. 6(b) shows normalized SNR plotted on a linear scale as a function of frequency for the 100-fs jitter case shown in Fig. 6(a). As is clear from Fig. 6, increasing the RF input frequency causes a decrease in the ENOB. There are also some peaks in the ENOB curve versus frequency in Fig. 6 which correspond to the system transfer function peaks. The results show that the frequency dependence of ENOB is proportional to the system transfer function divided by the frequency. Also from these simulations it is apparent that to obtain more than 6-b resolution at frequencies of 15 GHz and higher we would need an optical input jitter in which is less than 100 fs. Such a small value of jitter may be achieved using a recently introduced multiwavelength mode-locked semiconductor laser [4], [5].

The effect of detector shot noise on system performance with no jitter is shown in Fig. 7 for different detected optical power. The shot noise is added to the signal at the detector output and is calculated based on the average optical signal power in each
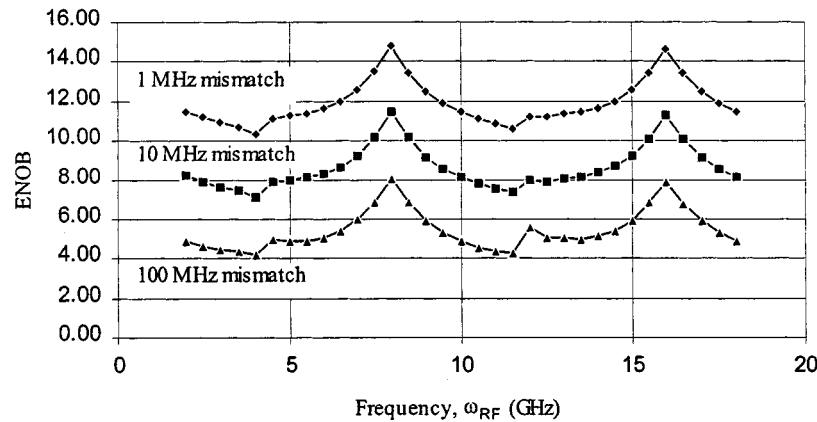
Fig. 9. The effect of single-channel LPF frequency mismatch on the frequency dependence of the ENOB. The five-channel system uses eight-pole Butterworth LPF's with 4-GHz −3-dB bandwidth. The simulation assumes no jitter and no shot noise.

channel. As expected, the frequency dependence of the ENOB is proportional to the system transfer function. To obtain 6-b resolution at frequencies of 15 GHz or higher, greater than a few milliwatts of average detected optical power per channel is required. This power is the detected optical power at the photodiode. The source optical power will be higher due to optical losses in the system.

Results of simulation show that shot noise is dominant at low frequencies and jitter noise is dominant at high frequencies. The jitter and shot noise sources are independent in the system and their contribution may be considered separately.

Fig. 8 shows the noise associated with a reconstructed 2-GHz signal. We find that noise amplitude due to jitter is directly proportional to the signal amplitude.

Amplitude and frequency mismatch in different channels exponentially reduce the EBOB if not compensated for. For example, a small difference in the power level in different channels will cause generation of spurious signals. In principle, this effect may be compensated for by dynamic or static calibration of the system using known signals. Fig. 9 shows the degradation in ENOB due to a single mismatched LPF in a system with no shot noise and no jitter. It is clear that even a small mismatch causes large degradation in system performance.

V. CONCLUSION

An optoelectronic WDM architecture and DSP can be used to enhance electronic ADC performance. The system architecture was analyzed and simulated. The analysis described in this paper shows that a five-channel system with 6-b resolution and 15-GHz −3-dB RF input bandwidth is achievable using a mode-locked laser source with less than 100-fs jitter and greater than 1-mW average received optical power per channel. The system makes use of simple, practical LPFs and 28-ps-wide optical pulses with low-amplitude noise. We find that performance of the hybrid WDM ADC system is sensitive to LPF frequency mismatch. In general, optimized WDM ADC performance requires balanced channel response. Our analysis quantifies the enhancement in WDM ADC performance that may be achieved by reducing jitter, increasing average received optical power, and tightly matching LPF frequency response. In this initial work, the noise terms are independent and additive. Our work may be considered a basic starting point for creation of future, more sophisticated, design tools for hybrid optoelectronic WDM ADC systems. We believe that a natural extension is to include the effects of nonlinear response.

REFERENCES

[1] H. F. Taylor, "An optical analog-to-digital converter-design and analysis," *IEEE J. Quantum Electron.*, vol. QE-14, pp. 210–216, Apr. 1979.
[2] A. Bhushan, F. Coppinger, and B. Jalali, "Time-stretched analogue-to-digital conversion," *Electron. Lett.*, vol. 34, no. 11, pp. 1081–1083, 1998.
[3] J. U. Kang and R. D. Esman, "Demonstration of time interweaved photonic four-channel WDM sampler for hybrid analogue–digital converter," *Electron. Lett.*, vol. 35, no. 1, pp. 60–61, 1999.
[4] P. J. Delfyett, H. Shi, S. Gee, C. P. J. Barty, G. Alphonse, and J. Connolly, "Intracavity spectral shaping in external cavity mode-locked semiconductor diode lasers," *IEEE J. Selected Topics Quantum Electron.*, vol. 4, pp. 216–223, Mar./Apr. 1998.
[5] H. Shi, I. Nitta, G. Alphonse, J. Connolly, and P. Delfyett, "Timing jitter performance of multi-wavelength mode-locked semiconductor laser," *Electron. Lett.*, vol. 34, no. 23, pp. 2250–2252, 1998.
[6] A. Yariv, *Optical Electronics.* New York: CBS College Publishing, 1985.
[7] C. Cox, E. Ackerman, R. Helkey, and G. Betts, "Techniques and performance of intensity-modulation direct-detection analog optical links," *IEEE Trans. Microwave Theory Tech.*, vol. 45, pp. 1375–1383, Aug. 1997.
[8] C. H. Cox, "Gain and noise figure in analogue fiber-optic links," *Proc. Inst. Elec. Eng. J.*, vol. 139, no. 4, pp. 338–242, 1992.
[9] M. J. Demler, *High-Speed Analog-to-Digital Conversion.* San Diego, CA: Academic, 1991.
[10] K. Hsu and C. M. Veber, "Stochastic mode-locking theory for external-cavity semiconductor lasers," *J. Opt. Soc. Amer. B*, vol. 8, no. 2, pp. 262–275, 1991.

Payam Rabiei, photograph and biography not available at the time of publication.

A. F. J. Levi, photograph and biography not available at the time of publication.